von Rad, U., Haq, B. U., et al., 1992
Proceedings of the Ocean Drilling Program, Scientific Results, Vol. 122

14. SEDIMENTARY CYCLES ON THE EXMOUTH PLATEAU[1]

Xenia Golovchenko,[2] Peter E. Borella,[3] and Suzanne O'Connell[4]

ABSTRACT

Sedimentary cycles are observed in the nearly complete Lower Cretaceous to Eocene pelagic carbonates at Site 762 on the Exmouth Plateau off northwest Australia. The high-frequency cycles of variable clay and foraminifers in nannofossil chalk appear as color cycles repeating on a scale of centimeters to meters in thickness. Measured cycle thickness indicate that the dominant cycles appear to be related to the precession and obliquity periods.

To evaluate the high-frequency variance observed on the gamma-ray curve, spectral analysis of the log was performed on two intervals: 260 to 365 mbsf in the Cenozoic, and 555 to 685 mbsf in the Mesozoic. Average Cenozoic sedimentation rates of 10.5 m/m.y. are high enough to show that variance is present in the full suite of eccentricity bands (413-123-95 k.y.). Spectral analysis of the Mesozoic section failed to produce dominant peaks that could be correlated to predicted orbital periods. The bioturbation observed in the cores in this interval may be responsible for diluting the signal and producing high-frequency noise, which is manifested in the spectra as low, broad amplitude peaks.

Orbital forcing may be affecting sedimentation on the Exmouth Plateau by influencing cycles of increased carbonate production or dissolution. Alternatively, clay abundance cycles may be related to eolian deposition during cycles of increased aridity in western Australia.

Four low-frequency events were also identified at Site 762 from the core and log data. The duration of these events is approximately 13 m.y., and the conformable boundaries of these sedimentary cycles correlate with observed nondepositional surfaces in other wells in western Australia. The causal mechanism for the onset of these events may be eustatic, but alternatively may be regional tectonism with associated circulation pattern changes.

INTRODUCTION

The northwest Australian margin is an old, sediment-starved continental margin. During the Late Cretaceous and Cenozoic, terrigenous sediment input was minimal, making this margin an excellent area to study the changes in sediment supply in order to test various causes of rhythmic sedimentation.

In summer 1988, the Ocean Drilling Program (ODP) initiated a study of the Northwest Shelf of Australia which included two drilling programs (designated Legs 122 and 123) using the drillship *JOIDES Resolution*. Two transects were drilled along this margin: across the central Exmouth Plateau, and across the Wombat Plateau (a subplateau of the Exmouth Plateau) and on to the Argo Abyssal Plain. This area, part of the Westralian Superbasin, forms a portion of Australia's continental margin (Veevers, 1988). Figure 1 shows the location of the six drill sites from Leg 122 (Sites 759 to 764) and one drill site from Leg 123 (Site 766). The cores from these sites record Late Triassic syn-rift to Cretaceous/Cenozoic post-rift sedimentation in the north (Wombat Plateau), to Neocomian syn-rift deltaic sedimentation and Aptian to Quaternary hemipelagic to eupelagic sedimentation in the south (central Exmouth Plateau). At the sites on the Wombat Plateau, we recovered extremely condensed Cretaceous and Cenozoic sections with numerous hiatuses (Shipboard Scientific Party, 1990). Cycles were rare at these sites and therefore difficult to analyze. Site 763 on the central Exmouth and Site 766 at the foot of the Exmouth Plateau Escarpment (Fig. 1) also contain hiatuses and several condensed sections, and therefore were not evaluated. At Site 762, we recovered a thick Cenomanian to Quaternary sequence of pelagic marls, chalks, and oozes (Fig. 2). Carbonate deposition at this site appears to be continuous except for a hiatus of approximately 3 m.y. at the Cretaceous/Tertiary boundary. Cycles of variable clay concentrations ranging from 6 to 200 cm were observed within the pelagic carbonates of Cenomanian to Eocene age at Site 762. These high-frequency cycles were also noted in the geophysical logs, especially the natural gamma-ray curve. In addition to these small-scale cycles, the cores and geophysical logs showed lower frequency events with thicknesses of approximately 100–150 m.

The purpose of this paper is to describe these observed cycles and events, and relate them, if possible, to extraterrestrial (Milankovitch, 1938) and/or intraterrestrial (tectonic, eustatic) phenomena.

LITHOSTRATIGRAPHIC OVERVIEW

Lithologies from Cores

Shipboard subdivision of the nannofossil chalk of Cenomanian through Eocene age discussed in this paper was based on the variations of foraminifers and clay percentages. The sedimentary sequence was divided into lithologic units on the basis of visual core descriptions, smear slide analysis of sediment composition, and calcium carbonate contents (Shipboard Scientific Party, 1990). The following lithostratigraphic overview is taken from the shipboard core description of Site 762 (Fig. 2).

Lithologic Unit II (181.5–265.0 meters below sea floor, or mbsf) consists of nannofossil chalk with no significant amount of siliciclastic material. No cyclicity was observed within this middle to late Eocene section.

[1] von Rad, U., Haq, B. U., et al., 1992. *Proc. ODP, Sci. Results*, 122: College Station, TX (Ocean Drilling Program).
[2] Borehole Research Group, Lamont-Doherty Geological Observatory, Palisades, NY 10964, U.S.A.
[3] Natural Science Division, Saddleback College, Mission Viejo, CA 92691, U.S.A.
[4] Department of Earth and Environmental Sciences, Wesleyan University, Middletown, CT 06547, U.S.A.

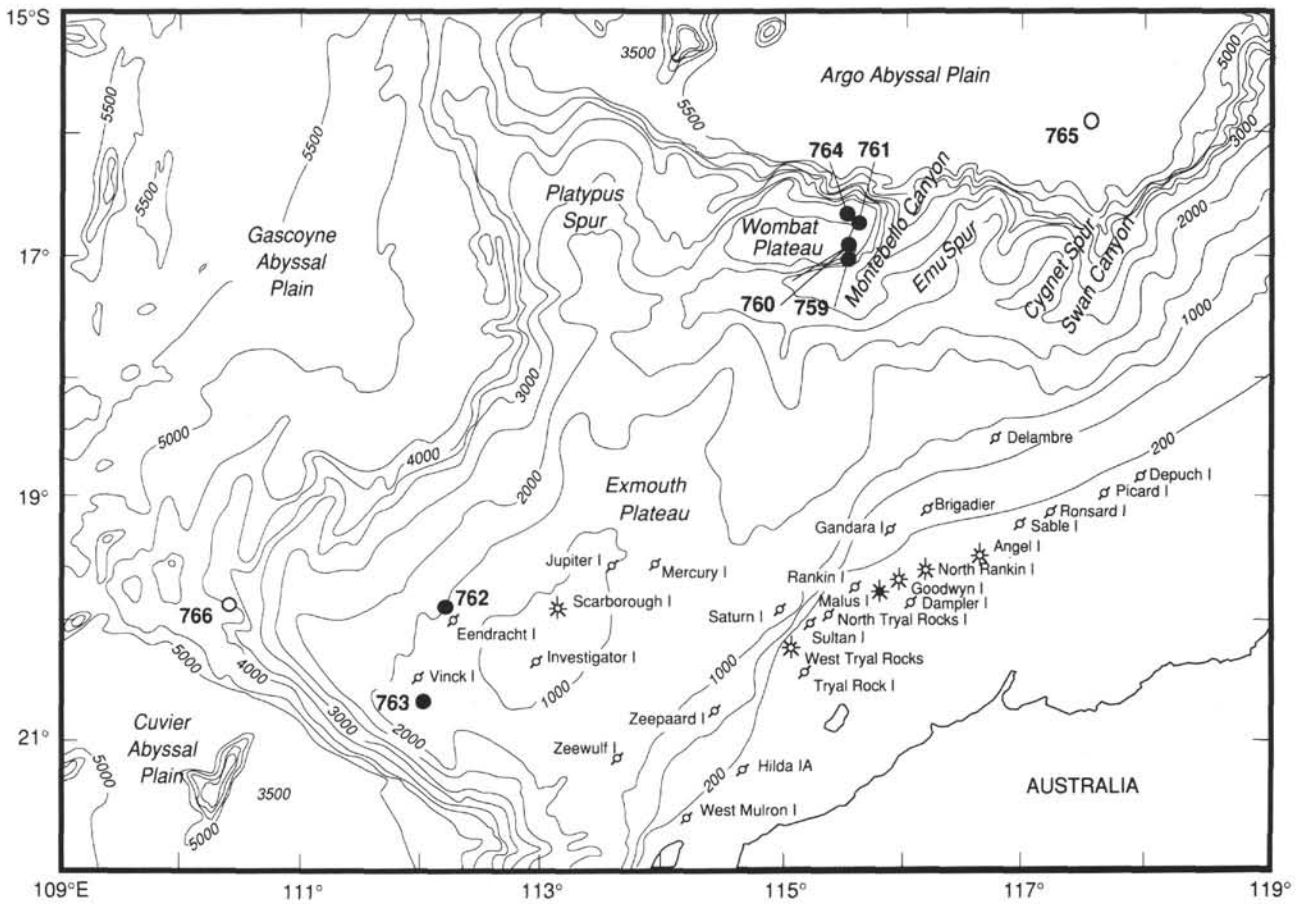

Figure 1. Site locations for Leg 122 off northwest Australia (from Shipboard Scientific Party, 1990). Bathymetry in meters.

Lithologic Unit III (265.0–554.8 mbsf) is subdivided into Subunits IIIA and IIIB based mainly on downhole variation in the amount of planktonic foraminifers, with Subunit IIIA consisting of nannofossil chalk with foraminifers, and Subunit IIIB dominated by nannofossil chalk. Both subunits display color cyclicity related to variations in foraminifers and clays. Subunit IIIA is 133 m thick and ranges in age from early Eocene to middle Eocene. Subunit IIIB is 157 m thick and is early Paleocene to early Eocene in age.

Lithologic Unit IV (554.8–838.5 mbsf) consists of nannofossil chalk with varying amounts of foraminifers, clay, and nannofossil claystones. The top of Unit IV is marked by the Cretaceous/Tertiary boundary, where the white nannofossil chalk of Unit IV overlain by the dark green-grey nannofossil chalk with foraminifers of Unit III.

Each of the five subunits of Unit IV is characterized by distinct color as well as compositional change. Each subunit also includes small-scale (5–100 cm) color cycles of darker and lighter beds. Subunit IVA, a white to light green-grey nannofossil chalk, contains thin green-grey beds consisting of clayey nannofossil chalk. This subunit, of early to late Maestrichtian age, is 48.7 m thick. Subunit IVB, a brown interval, consists of nannofossil chalk with varying amounts of clay occurring in beds 35–130 cm thick. The subunit is 93.5 m thick and ranges in age from early Campanian to late Maestrichtian. Subunit IVC (697.0–780.0 mbsf), a green interval, consists of nannofossil chalk with varying amounts of foraminifers and clay, which form 10- to 80-cm-thick layers. This subunit is early Santonian to early Campanian in age. Subunit IVD (780.0–820.2 mbsf) is a brown interval of foraminifer nannofossil chalk of late Albian to early Santonian age. The Cenomanian/Turonian boundary lies within this interval. Gradational cyclic color changes on the order of 10–85 cm were noted in this subunit. Subunit IVE (820.2–835.5 mbsf) is a green interval of Albian age representing the onset of hemipelagic sedimentation during the "juvenile ocean stage" (von Rad et al., 1989). Subunit IVE consists of clayey calcareous chalk and nannofossil chalk with clay. Intervals of alternating light green-gray to green-gray beds are 15–110 cm thick. However, the contacts between beds are gradational and contain many bioturbation structures.

The color banding observed in Units III and IV is evaluated later in this paper for dominant periodicities and correlation with known cyclic events.

Lithologies from Wireline Logs

The first lithologic unit sampled by the logging tools was Unit II (187–265 mbsf) at 196 mbsf (Fig. 3). The log character is fairly monotonous over this interval, as would be expected in nannofossil chalk with no appreciable amounts of siliciclastic material.

The pattern of change between nannofossil chalk and increased amounts of detrital material in Units III (265.0–554.8 mbsf) and IV (554.8–838.5 mbsf) in Hole 762C is easily detected on the gamma-ray log. The log, which is tied to the core depths on the basis of the distinct log response at the Cretaceous/Tertiary boundary, clearly defines the lithostratigraphic unit boundaries and the changes in facies within the units. High and low frequency variations in calcium carbonate concentrations are quite apparent on the gamma-ray log (Fig.

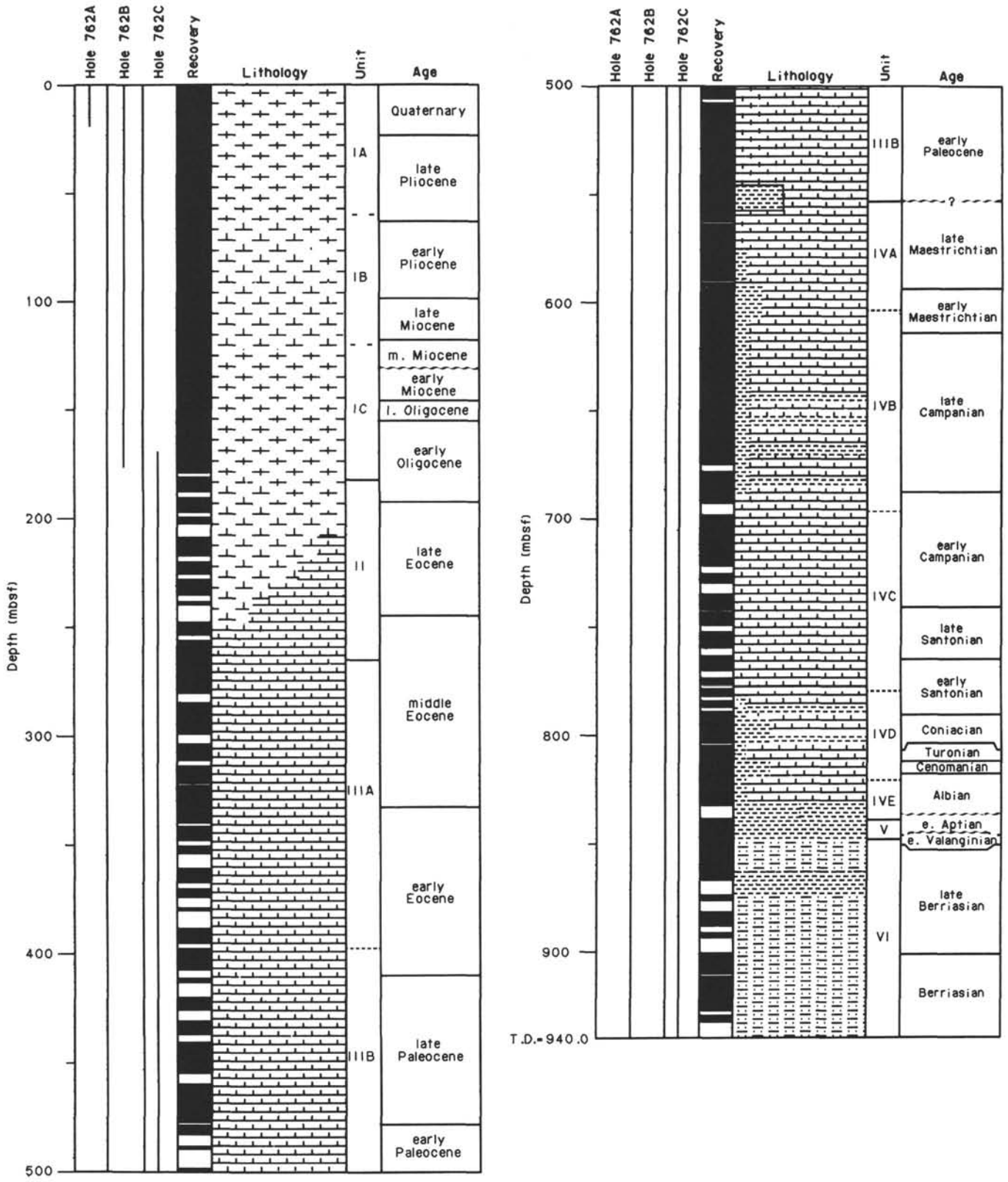

Figure 2. Lithologic column for Site 762 showing generalized lithology, lithologic units, recovery, and age (from Shipboard Scientific Party, 1990).

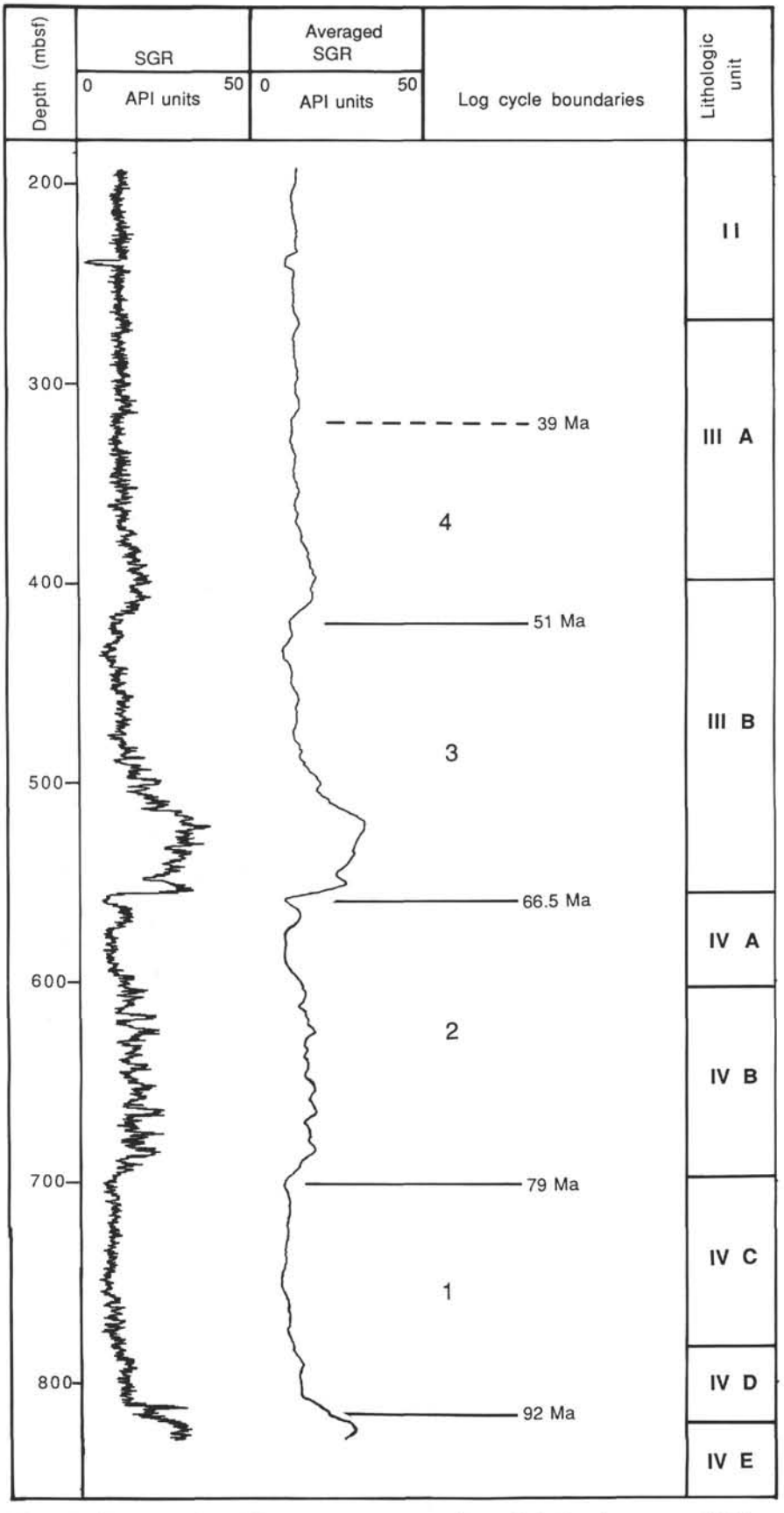

Figure 3. Gamma-ray log (left), gamma-ray curve with applied 43-point average (right) to show low-frequency cycles, and lithostratigraphic units. Cycle boundaries are based on baseline shifts in the gamma ray counts; ages are extrapolated from the shipboard sedimentation rates (Shipboard Scientific Party, 1990). SGR = spectral gamma ray.

Table 1. Matrix tabulation of Cenozoic cycle thickness (cm) vs. core number, Site 762.

Core 122-762C-	6–15	16–25	26–35	36–45	46–55	56–65	66–75	76–85	86–95	96–105	106–115	116–125	126–135	136–145	146–155	196–205	216–225	Total
17X	0	1	1	5	0	1	0	0	0	0	1	0	0	0	0	0	0	9
18X	0	0	0	0	0	0	0	0	0	0	0	2	0	0	0	0	0	2
19X	0	0	1	1	0	2	1	0	1	0	0	0	0	0	0	0	0	6
20X	0	1	0	0	1	1	0	0	1	0	0	0	0	0	0	0	0	4
22X	0	0	0	0	0	1	0	0	0	0	0	0	0	0	0	0	0	1
23X	0	0	2	0	0	0	0	1	0	0	0	0	0	0	0	0	0	3
24X	0	0	0	0	0	0	0	0	1	1	0	0	0	0	0	0	0	2
25X	0	0	0	0	0	0	0	0	0	0	0	1	0	0	0	0	0	1
26X	0	0	0	2	1	0	0	0	0	0	0	1	1	0	0	0	0	5
28X	0	0	1	1	0	0	0	0	0	1	0	0	0	0	0	0	0	3
29X	0	0	0	1	0	0	0	0	0	0	0	0	0	0	0	0	0	1
31X	1	8	5	2	0	1	0	0	0	0	0	1	0	0	0	0	0	18
32X	0	0	0	0	0	0	0	0		0	1	0	0	0	0	0	0	1
33X	0	3	4	2	0	1	0		0	0	1	0	0	0	0	0	0	11
34X	0	0	1	0	0	1	0	0	0	1	0	0	1	0	0	0	1	5
35X	0	1	1	0	1	0	0	0	0	0	0	0	0	0	0	0	0	3
38X	0	0	0	0	0	0	0	0	0	0	0	0	1	1	0	0	0	2
42X	0	0	0	0	0	0	0	0	0	0	0	0	0	0	1	1	0	2
	1	14	16	14	3	8	1	1	3	3	3	5	3	1	1	1	1	79

3), which is sensitive to changes in the relative abundance of clay-rich material and heavy minerals.

SEDIMENTATION RATES

Critical to the identification of cycle periodicities and causal mechanisms is an accurate determination of sedimentation rates. Estimation of sedimentation rates at Site 762 was based on calcareous nannofossil stratigraphy using the time scale of Haq et al. (1987). The sedimentation rates at this site are not well constrained and can be in error by as much as 50% due to poor biostratigraphic zonation, productivity dissolution, dilution, and differential compaction between carbonate and clay-rich layers (see "Biostratigraphy" and "Physical Properties" sections, "Site 762" chapter, Shipboard Scientific Party, 1990; T. Bralower, pers. comm., 1990).

No Mesozoic nannofossil zonation has yet been developed that has worldwide applicability, and this was especially evident on the Exmouth Plateau. Mesozoic zonations of Sissingh (1977) and Roth (1978) were not applicable in numerous intervals at Site 762 because of the absence of markers, and different order of events observed. Therefore, zonations at this site show the relative sequence and age of the events in the Mesozoic, but not their exact stratigraphic position ("Explanatory Notes" chapter, Shipboard Scientific Party, 1990). Nannofossil zonation schemes for the Cenozoic were those of Martini (1971).

Minimum average rates of sedimentation can be estimated by assuming continuous deposition across the geologic stages determined by the biostratigraphy. The average sedimentation rate calculated for lithologic Unit III (middle Eocene to early Paleocene) is about 10.5 m/m.y. The minimum average sedimentation rate for Unit IV from 554.8 mbsf (late Maestrichtian) to 682.0 mbsf (late Campanian) is 14.1 m/m.y. From 682.0 to 793 mbsf (early Santonian) the calculated average sedimentation rate is 12.3 m/m.y.

MILANKOVITCH CYCLES

Milankovitch cycles with predicted periods of variation of precession (19,000–23,000 yr), obliquity (42,000 yr), and eccentricity (95,000–123,000 and 413,000 yr) affect the seasonal and annual solar insolation, producing long-term global and hemispheric climates (Milankovitch, 1938; Imbrie and Imbrie, 1979) and oceanographic processes (Hayes et al., 1976).

In pelagic deep-sea sediments, $\delta^{18}O$ of biogenic carbonate and calcium carbonate concentration (an indicator of the balance between paleoproductivity, dissolution, and/or dilution by other components) are the parameters most commonly measured to detect Milankovitch frequencies. However, sedimentary responses are detectable in a wide variety of parameters that are commonly measured in both core and logs. These include clay type and abundance, grain size, mineral type and abundance, and porosity. Sedimentary responses to orbital forcing may differ from one location to another. For example, cycles of surface temperature or upwelling may cause variations in the biogenic components in one region, while aridity/humidity cycles may cause fluctuation in clay mineralogy or clay abundance in another region. Thus, a comprehensive analysis of mineralogical and physical changes in the sediment from core and log data is necessary for the detection of orbitally induced Milankovitch cycles in any sedimentary sequence.

CORE AND LOG ANALYSIS

Cyclicity in Cores

The initial core barrel sheets and photographs for Site 762, Cores 122-762C-17X through -61X were visually examined. Repeating couplets were measured and total thickness of the cycle was recorded. Cycle boundaries were based on color changes that repeated more than once within each section or between sections that were completely full with no missing intervals. Accuracy of measurement was within 1–3 cm. More than 300 cycles of varying thicknesses (6–225 cm) were measured within the Upper Cretaceous through Paleocene interval. Cycle thickness was then grouped into 10-cm intervals and plotted against core number (depth) (Tables 1 and 2). Histograms were then produced for the Cenozoic and Mesozoic sections (Figs. 4 and 5).

Cores 122-762C-17X through -42X are Cenozoic in age (middle Eocene to early Paleocene) and contain small cycles repeating on the scale of centimeters to meters in thickness. Color cycles alternate within this pelagic chalk interval with shades of green gray (10Y8/1 and 10Y8/2) and pale green (67/2, SG7/1) dominating toward the top of the interval, with light green-gray to very light green-gray beds becoming more apparent toward the bottom. Sometimes thin white bands are

Table 2. Matrix tabulation of Mesozoic cycle thickness (cm) vs. core number, Site 762.

122-762C-	6–15	16–25	26–35	36–45	46–55	56–65	66–75	76–85	86–95	96–105	106–115	126–135	166–175	266–275	Total
45X	0	0	0	2	2	4	0	1	0	0	0	0	0	0	9
46X	1	1	2	1	0	0	2	0	0	0	0	0	0	0	7
47X	3	7	9	1	0	0	0	0	0	0	0	0	0	0	20
48X	2	6	7	5	1	0	0	1	0	1	0	0	0	0	23
49X	2	6	4	3	0	0	1	0	0	0	0	0	0	0	16
50X	4	5	4	1	0	0	1	0	0	0	0	0	1	0	16
51X	1	3	2	0	2	3	1	1	0	1	1	0	0	1	16
52X	0	3	1	5	4	3	1	0	1	0	0	0	0	0	18
53X	2	5	5	4	2	1	1	0	0	0	0	0	0	0	20
54X	0	4	3	1	1	2	3	1	2	0	0	0	0	0	17
55X	1	3	1	2	1	1	0	1	0	0	0	0	0	0	10
56X	1	3	5	3	1	1	0	0	0	0	0	0	0	0	14
57X	0	0	0	0	0	1	1	0	0	0	0	0	0	0	2
58X	1	3	2	1	0	0	0	1	2	1	0	1	0	0	12
59X	5	6	2	1	2	0	0	0	0	1	0	0	0	0	17
61X	2	3	3	0	0	0	0	0	0	0	0	0	0	0	8
	25	58	50	30	16	16	11	6	5	4	1	1	1	1	225

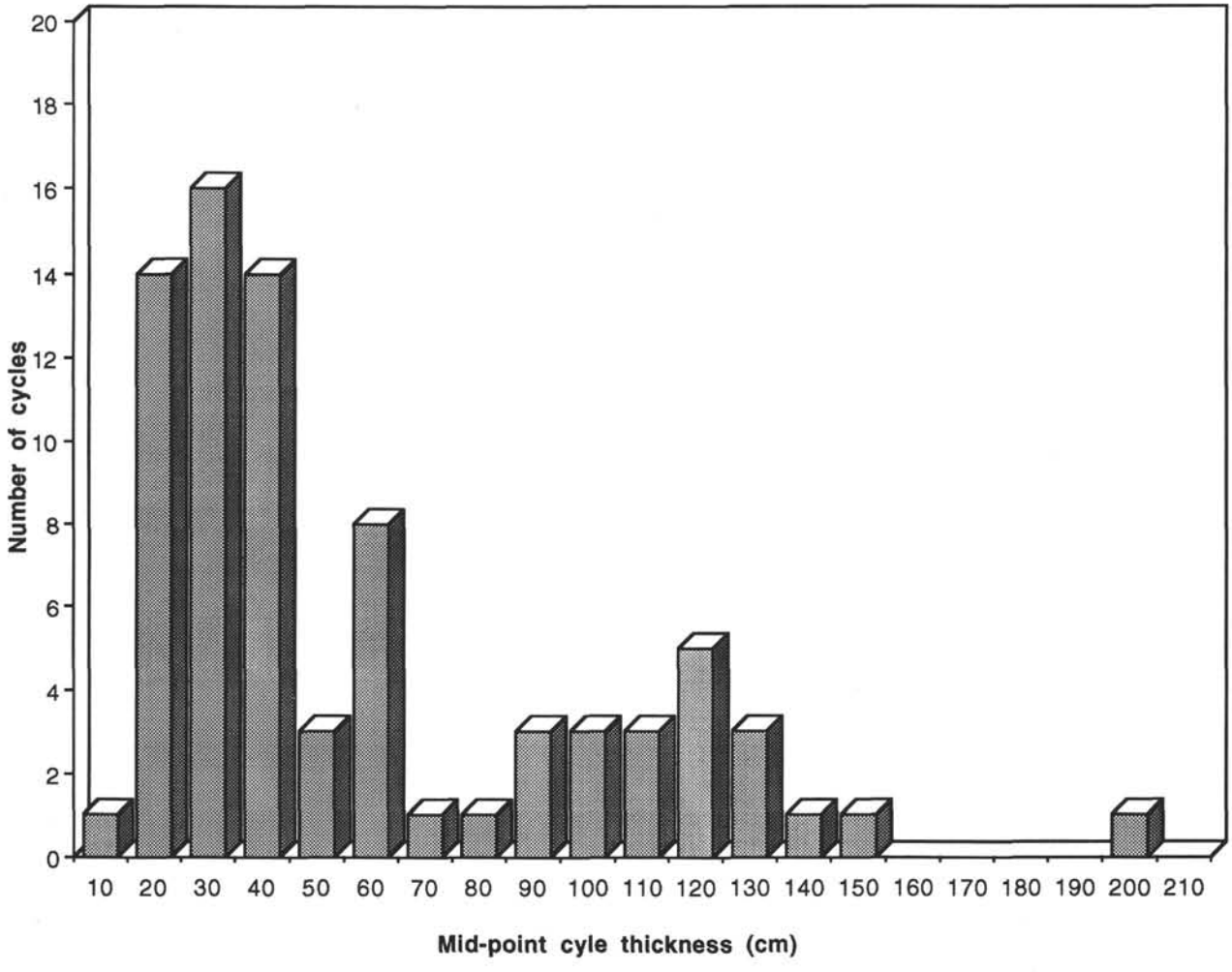

Figure 4. Histogram plot of frequency of cycle thickness, Cenozoic interval, Site 762.

observed that separate cycles (e.g., Cores 122-762C-29X, -30X, and -32X). Smear slide and calcium carbonate analyses indicate that the darker layers contain relatively more foraminifers and clay minerals. The alternation from foraminifer-rich to foraminifer-poor layers is most likely a function of dilution relative to nannofossils, dissolution rates, bottom-current activity, productivity, or some combination of these factors. The color variation also appears to be directly related to clay content (terrigenous or organic) and is a reflection of the original depositional environment (see Huang et al., this volume).

Results of our matrix tabulation (Table 1) and histogram (Fig. 4) for the Cenozoic interval indicate the dominant cycle thickness is between 20 and 40 cm. Sedimentation rates for

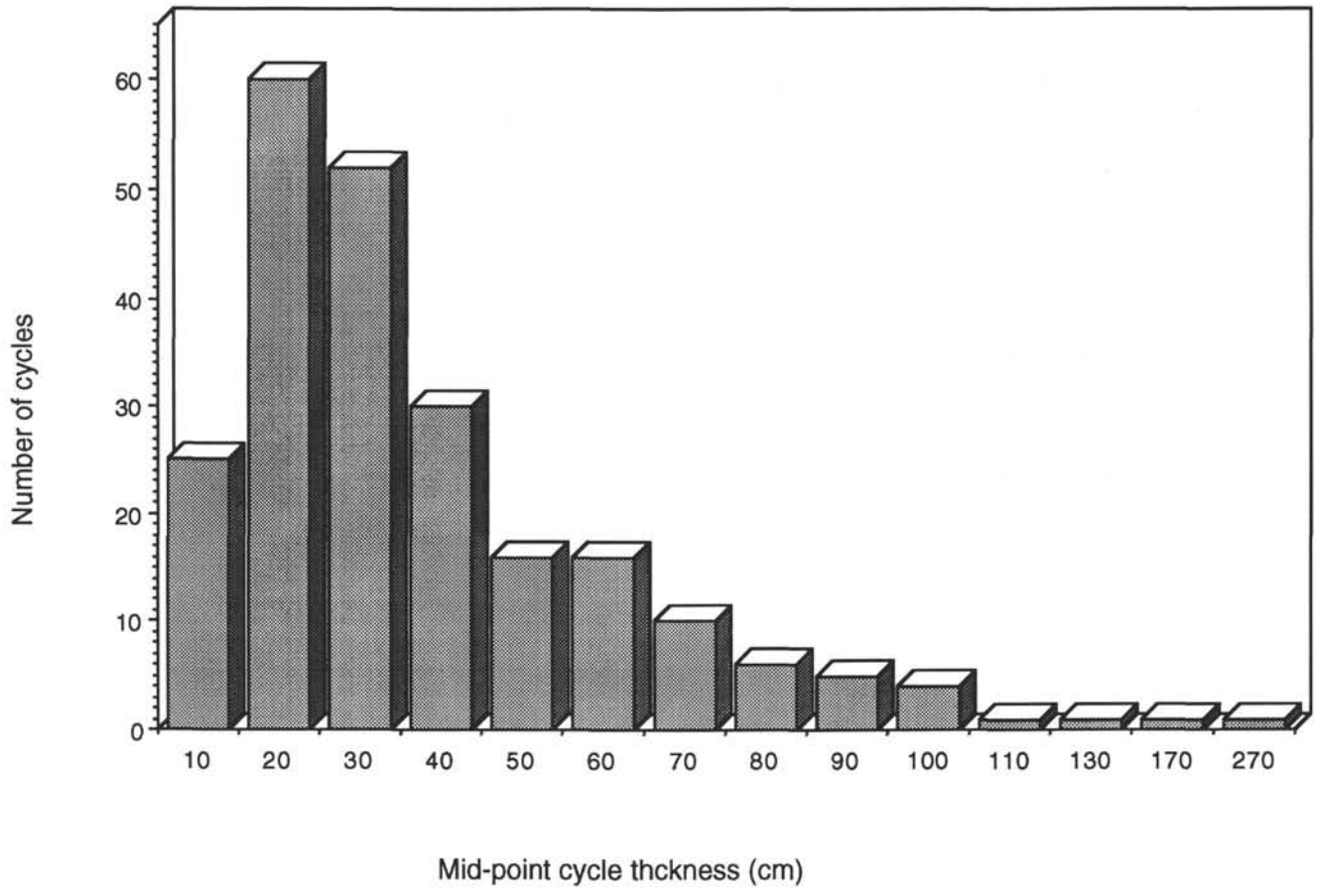

Figure 5. Histogram plot of frequency of cycle thickness, Mesozoic interval, Site 762.

this interval average approximately 10.5 m/m.y., yielding periods of precession and obliquity for these Cenozoic color cycles.

Two other cycle thickness peaks are present at 55–65 cm and approximately 116–125 cm. Applying the same sedimentation rate, these cycles would yield cycle durations of 57,000 and 114,000, respectively. These cycles do not appear to correspond to any known periodicities. However, these peaks may actually be multiples of the 16–25 cm and 26–35 cm cycles, which would explain the lack of correlation with Milankovitch frequencies.

The chosen Mesozoic intervals (Cores 122-762C-45X to -61X) show similar cyclic events (Table 2 and Fig. 5). Color-alternating nannofossil chalks with varying amounts of foraminifers and clay dominate this Upper Cretaceous interval, which is bounded by the Cretaceous/Tertiary boundary at the top (554.8 mbsf) and the Cenomanian/Turonian boundary at the bottom (810.0 mbsf). The cores are within the lithologic Unit IV that is further divided into five subdivisions based on large-scale 10- to 100-m-thick color changes. Located within each of these subdivisions are small-scale cyclic color patterns that have couplet thicknesses ranging from 6 to 270 cm. The dominant cycle thickness is between 15 and 45 cm (Fig. 5), again averaging around 25–30 cm.

Couplet colors in uppermost Subunit IVA (554.8–603.5 mbsf) (upper green interval) are white (25Y8/0) alternating with light green-gray (5GY7/1). The lighter beds include up to 15% foraminifers with the darker beds having 3%–20% more clay. Calcium carbonate content in the lighter beds is 87%–92%, whereas the darker beds have only 56%–92%. Bioturbation is moderate to strong, making the boundaries gradational. Couplet thicknesses ranges from 10 to 100 cm.

Subunit IVB (603.5–697.0 mbsf) consists of sedimentary cycles ranging in thickness from 10–270 cm. Colors range from red-brown (5YR5/3) through light red-brown (5YR6/3) to white (10YR8/1). The darker beds (red and red-brown) contain on the average 1%–27% more clay and 3%–10% more iron oxides than the lighter beds. Bioturbation is strong and burrowing has locally mixed lighter and darker intervals. Foraminifer content is variable, ranging from 4%–20% or greater.

Subunit IVC (Cores 122-762C-58X to -69X) is a green interval consisting of alternating white (5Y8/1) to very light green-gray (10Y8/1) nannofossil chalks with green-gray (5G5/1) nannofossil claystones. Couplet thicknesses range from 20 to 125 cm (Table 2). Calcium carbonate content is 89%–94% in the lighter beds and 36%–67% in the darker intervals. Bioturbation is moderate and the nannofossil claystones are finely laminated, commonly showing both sharp and gradational upper and lower contacts.

Subunit IVD (780–820.2 mbsf) is the lower brown interval and Subunit IVE is the lower green interval. Both of the intervals contain cyclic sedimentation beds that are very similar to those already described. A detailed analysis of these cycles was not made because of the condensed sequence observed at the Cenomanian/Turonian boundary (Subunit IVD) and the change in sedimentation regime from pelagic to hemipelagic (Subunit IVE). Sedimentation rates are highly variable within these intervals.

Sedimentation rates for Subunits IVA–C are approximately 14 m/m.y. The most frequently occurring cycle is between 15

and 35 cm thick. This gives a couplet age ranging from 10,700 to 25,000 yr, which agrees fairly well with the 20,000-yr precession cycle. Of the 225 cycles measured in this interval, 163 cycles were 45 cm thick or less. Forty-three cycles were observed that had couplet thicknesses from 46 to 75 cm, averaging approximately 60 cm or about 42,000 yr in duration. These data agree well with the observations in the Cenozoic section and indicate that the 20,000-yr precessional cycle is recorded in these sedimentary sequences. These cycles also transgress major geologic era boundaries (i.e., the Cretaceous/Tertiary boundary) and indicate that the cause of these small-scale cycles are independent of causes that produced major geologic boundaries and/or events. Similar couplet thicknesses with 20,000-yr cycles or multiples thereof have been found in the southern oceans and are discussed elsewhere (Borella, 1984; Dean et al., 1978).

Spectral Analysis of the Gamma-Ray Log

Reconnaissance spectral analysis was performed on the gamma-ray log in two separate depth intervals: 250.0–365.0 mbsf and 554.8–685.0 mbsf. The upper interval was chosen as a representative Cenozoic section in Hole 762C. The upper limit of the second interval corresponds to the Cretaceous/Tertiary boundary where the log makes a sharp baseline change, and the lower limit was chosen because of poor biostratigraphic constraints below this horizon. The natural gamma-ray log was selected for the analysis because it is commonly used to indicate downhole variations in clay mineral content, and may therefore act as an indicator of terrigenous or eolian component within the nannofossil chalk. The log reflects total gamma radioactivity from potassium (K), thorium (Th), and uranium (U) decay, the first two of which are common elements in clay minerals, whereas uranium abundance can be strongly correlative with organic carbon content (Rider, 1986).

The log data were converted from the depth domain to the frequency domain via spectral analysis. The technique applied to this data set is described in detail in Molinie and Ogg (unpubl. data). The analysis was applied to the intensity fluctuations of the recorded natural gamma ray in Hole 762C. The gamma-ray data were recorded every 15.24 cm with vertical resolution limited to about 45 cm. Assuming a sedimentation rate of 15 m/m.y., the maximum cycle resolution would be greater than 42,000 yr (obliquity).

In order to obtain a time-series analysis of the gamma-ray log, we normalized the data within the chosen intervals to assure numerical stability in the calculation. The normalization procedure removes the dominating zero-order term, associated with the non-zero mean of the log data, that would otherwise be present in the amplitude spectrum.

A low-pass filter of 1.5 cycles/m was applied to the data set in order to remove all high-frequency noise. This low-pass filter also eliminates the problem of aliasing caused by the Nyquist frequency, which is a function of the sampling frequency. Since the gamma-ray readings are recorded every 15.24 cm, the corresponding Nyquist frequency is 6.56 cycles/m, and the cut-off filter has a frequency equivalent to the Nyquist frequency divided by four, or 1.5 cycles/m. Harmonics of the Nyquist frequency may still be present as multiples of 6.56 cycles/m, but these signals will have reduced amplitudes.

The analysis was applied on a series of closely-spaced, overlapping, sliding windows to resolve the power spectra. The 40-m sliding window corresponds to approximately 260 data points. To eliminate discontinuities across the truncated window, a multitaper analysis method (Thompson, 1977) was used to calculate spectra at each selected depth window. This technique minimizes the spectral leakage, and also prevents the omission of data in the chosen window. For this analysis, we used a combination of five tapers of different shape. This allows information discarded by the first taper to be partially recovered by the higher order tapers. To calculate the spectra for the gamma-ray curve, the multitaper spectral technique was applied to the normalized log within a sliding 40-m window moved at regular 1.0-m intervals. The spectra within this window are calculated by using the Fourier transform of each tapered log.

SPECTRAL ANALYSIS RESULTS

Results of the spectral analysis are presented at selected depths as amplitude of frequency components vs. depth (Figs. 6 and 7). The predicted location of specific Milankovitch frequencies on the amplitude spectrum is determined by:

$$\text{[window length (m)/sedimentation rate (m/m.y.)]/ orbital frequency} = \text{predicted frequency} \quad (1.1)$$

If the major low-period peak is assigned as 413 k.y., then the corresponding "tuned" periods of the other eccentricity peaks should correspond to other spectral peaks. Using a sedimentation rate of 11.5 m/m.y. in the Cenozoic section (260–365 mbsf), peaks corresponding to 123 k.y. and 95 k.y. lie fairly close to the expected locations of these eccentricity cycles. These three peaks are consistently present with similar ratio (Table 3) in each of the depth windows despite apparent changes in sedimentation rates near the top of the interval. These fairly constant ratios between the three peaks, as well as their agreement with the estimated ratio for the three eccentricity peaks, confirms our assumption that eccentricity periods are indeed being observed.

The peaks of the power spectra in the Cenozoic interval change in intensity and width (Fig. 6), implying a gradual change in sedimentation rates has occurred in the lower part of this interval.

In the Mesozoic interval (Fig. 7), adjusting the periods of the other eccentricity cycles based on the location of the 413-k.y. peak does not appear to correlate with major peaks in the power spectra, and the ratios of probable eccentricity peaks (Table 4) are not consistent with the estimated ratios. The color cycles observed in the core correspond mainly to time durations of about 42 k.y. and 20 k.y., with no predominant cycles that can be related to eccentricity periods. This observation has been confirmed by Huang et al. (this volume).

It is interesting to note the types of Milankovitch periods observed in the core vs. log data. Core cyclicity was noted on the order of 15–65 cm, corresponding to precession and obliquity cycles. Log data, because of the low vertical resolution, were unable to differentiate cycles with periods less than ~50,000 yr and therefore were only able to detect the three eccentricity cycles. Yet all the Milankovitch cycles appear to be expressed in the Cenozoic sedimentary record of Site 762.

The orbital forcing function appears to be influencing the carbonate production or dissolution cycles associated with increased foraminifers and/or nannofossil dissolution. The cyclic variations in clay abundances imply a climatic control, such as changes in aridity/humidity, which controls the input of terrigenous material from western Australia.

LOW-FREQUENCY EVENTS

Observed on the gamma-ray log and in the cores are large-scale, low-frequency events (Fig. 3). These events are most noticeable from approximately the Cenomanian/Turo-

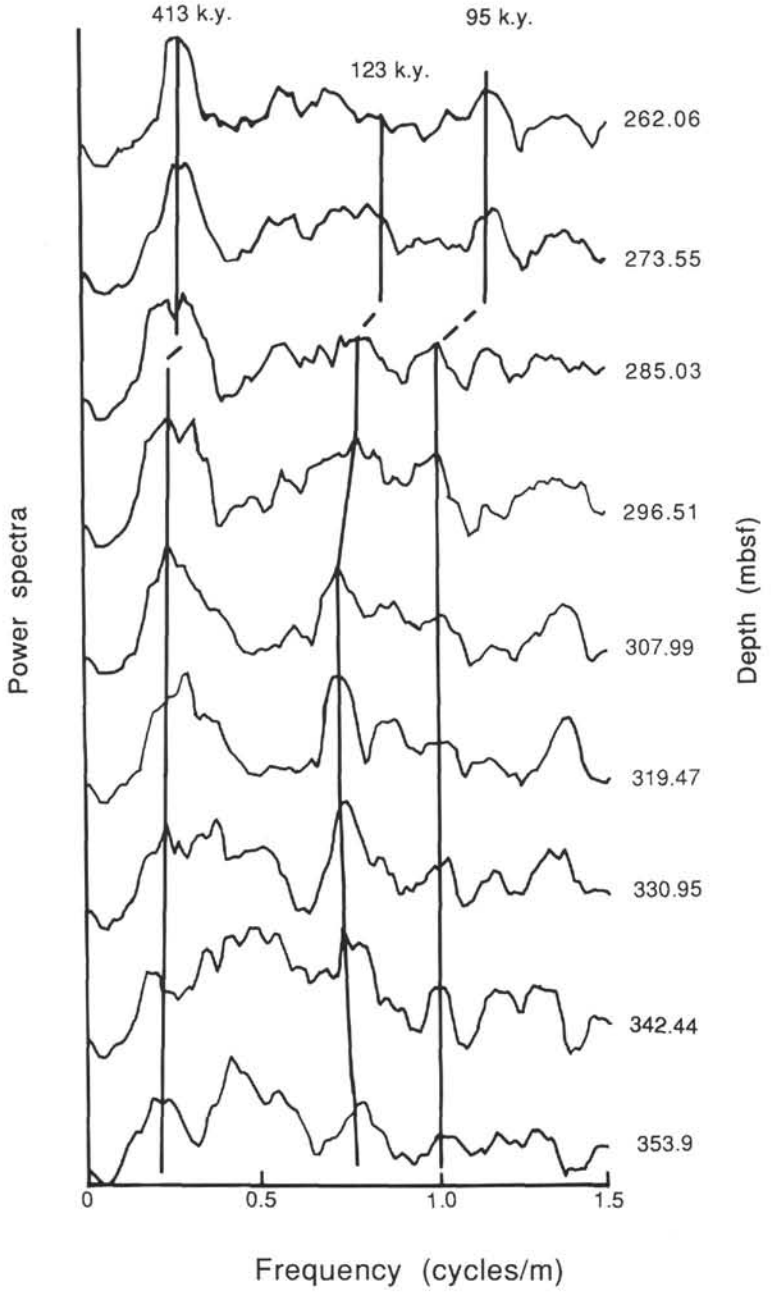

Figure 6. Selected spectra in the Cenozoic interval as a function of depth.

nian contact (810 mbsf) through the Cretaceous/Tertiary boundary (554.8 mbsf) and into the Paleocene to approximately 425 mbsf, and from the Paleocene to the late Eocene at approximately 273 mbsf. In the core the low-frequency couplets are distinguished on the basis of color change. These cycles showed a dominant color, grouping a dominant brown and green interval into a single couplet. In the Cenozoic portion, colors are green-gray alternating with light green-gray and white beds. The Mesozoic section consists of repeating brown and green intervals (see "Summary" section, "Site 762" chapter, Shipboard Scientific Party, 1990).

Depending on the sedimentation rate chosen, the duration of these low-frequency events ranges from 8–19 m.y. with an average duration of 13 m.y. It should be noted that a condensed section and an unconformable boundary were recognized at the Cenomanian/Turonian and Cretaceous/Tertiary boundaries, respectively (Shipboard Scientific Party, 1990). Sedimentation rates, as well as missing sections, make thickness and duration estimates difficult.

Correlation with clay content (color) and the gamma-ray log is excellent if the problematic areas around the Cenomanian/Turonian and Cretaceous/Tertiary boundaries are eliminated. The brown-colored part of the couplet contains more clay and relatively higher gamma readings compared to the green member that has less clay and lower gamma-ray counts.

Four low-frequency events were recognized at Site 762 (Fig. 3). The stratigraphically lowest event begins just beneath the Cenomanian/Turonian boundary at 830 mbsf (92 Ma) and ends at 697 mbsf (79 Ma). The duration of this event is 13 m.y. The second event begins at 697 mbsf (79 Ma) and ends at 554.8 mbsf at the Cretaceous/Tertiary boundary (66.5 Ma); it has a duration of 13.5 m.y. The third event begins at the Cretaceous/

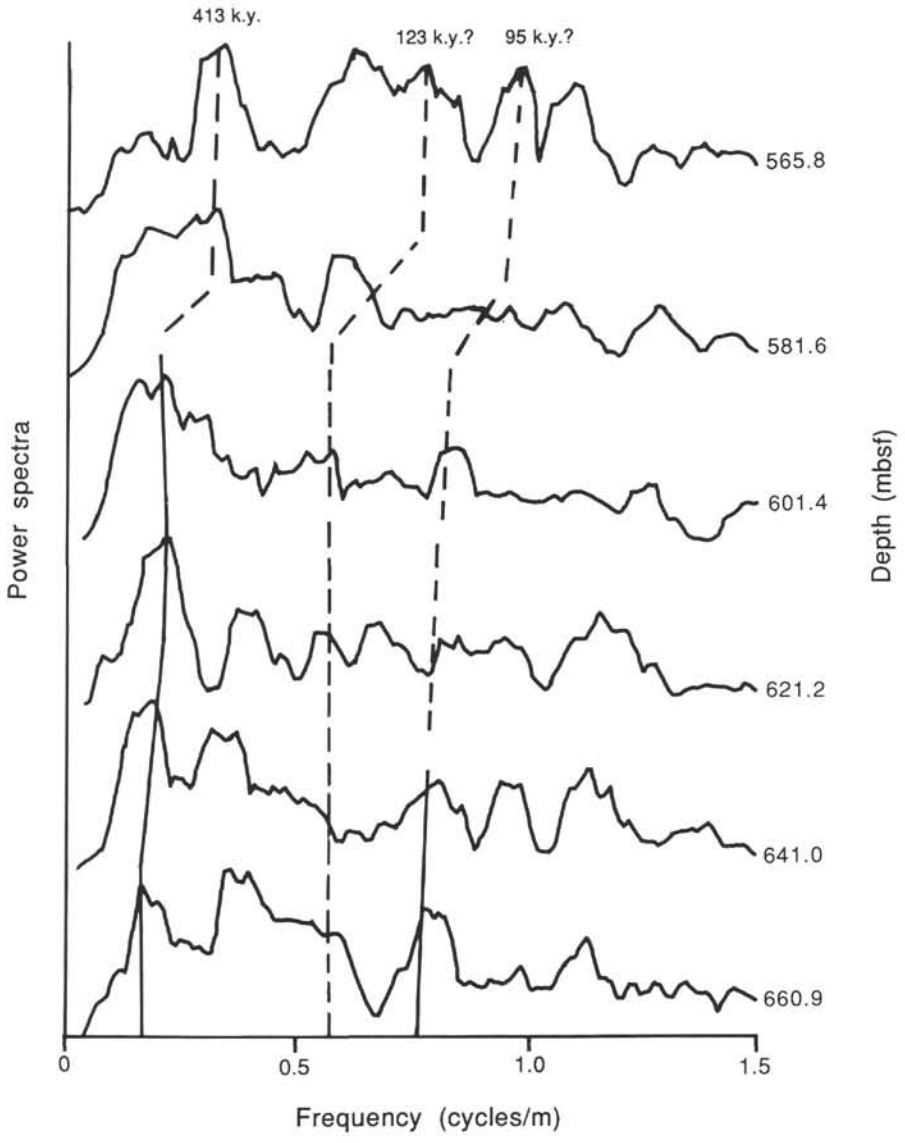

Figure 7. Selected spectra in the Mesozoic interval as a function of depth.

Table 3. Summary of the significant frequencies (in cycles/m) and corresponding ratios of spectral peaks showing optimal matches with 413, 123, and 95 k.y.

Depth (mbsf)	413 k.y.	123 k.y.	95 k.y.	413/123	413/95	125/95
262.1	0.29	0.82	1.13	0.35	0.25	0.72
273.5	0.29	0.82	1.13	0.35	0.25	0.72
285.0	0.24	0.78	1.02	0.32	0.23	0.76
296.5	0.21	0.74	0.97	0.28	0.21	0.76
308.0	0.21	0.74	0.97	0.28	0.21	0.76
318.5	0.21	0.74	0.97	0.28	0.21	0.76
330.9	0.21	0.74	0.97	0.28	0.21	0.76
342.4	0.21	0.74	0.97	0.28	0.21	0.76
353.9	0.21	0.74	0.97	0.28	0.21	0.76
			Expected ratios:	0.3	0.23	0.77

Note: Milankovitch eccentricity cycles in the Cenozoic interval.

Table 4. Summary of the significant frequencies (in cycles/m) and corresponding ratios of spectral peaks showing optimal matches with 413, 123, and 95 k.y.

Depth (mbsf)	413 k.y.	123 k.y.	95 k.y.	413/123	413/95	125/95
565.8	0.33	0.62	?	0.53	—	—
581.6	0.31	0.59	?	0.52	—	—
601.4	0.22	0.57	0.81	0.38	0.27	0.70
621.2	0.22	0.57	0.76	0.38	0.28	0.75
641.0	0.22	0.57	0.76	0.38	0.28	0.75
660.9	0.22	0.57	0.76	0.38	0.28	0.75
			Expected ratios:	0.29	0.22	0.77

Note: Milankovitch eccentricity cycles in the Mesozoic section.

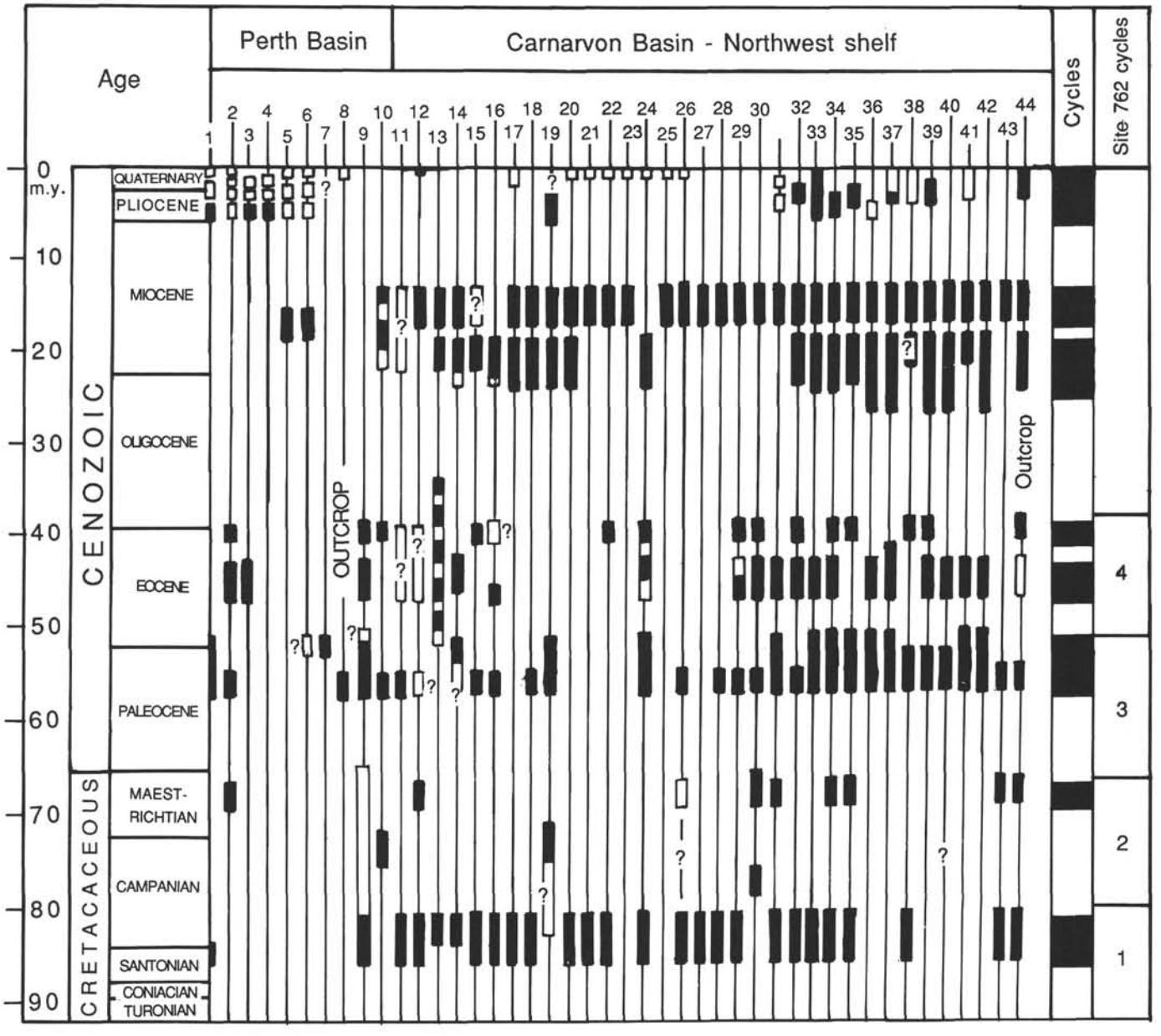

Figure 8. Hiatuses (black lines) identified in wells from western Australia, including Site 762 (after Quilty, 1980).

Tertiary boundary and ends at 415 mbsf (51 Ma), with a duration of 14.5 m.y. The fourth event begins at 415 mbsf and ends at 273 mbsf (39 Ma) after lasting 12 m.y. The cycle boundaries observed do not appear to be associated with significant changes in sediment accumulation rates.

The event boundaries are distinguished on the gamma-ray log by an increase in gamma-ray counts (API units) (Fig. 3). The first log event begins with an increase in gamma ray from 10 to 15 API units, which gradually decreases to an average of 5 API units. The second event begins with a change in API units from 5 to 12 and again the gamma-ray count gradually decreases to an average of 5 API units. The third sedimentary cycle begins with an increase from 4 to 28 API units and the fourth with an increase from 4 to 8 API units. Again, the gamma-ray counts gradually decrease to 4–5 API units over the span of the event (approximately 110–140 m).

The event boundaries observed at Site 762 correlate well with the ages of hiatuses, or periods of nondeposition, determined from well data off western Australia (Quilty, 1977, 1980) (Fig. 8). Within an error of 1 or 2 m.y., the time of nondeposition in wells on the continental margin and on shore correlate with the event boundary ages at Site 762 in the Campanian (~80 Ma), late Maestrichtian (~67 Ma), early Eocene (51 Ma), and late Eocene (39 Ma), demonstrating the cause of the event to be widespread. The same events however, have not been noted in the Gippsland Basin off southern Australia (Fig. 9).

A comparison of the ages of the sedimentary cycle boundaries to the hiatuses bounding the supercycles of Haq et al. (1987) shows there is a good match between them (Fig. 9). The cause of these events noted at Site 762 and elsewhere in western Australia may therefore be eustatic. However, it is

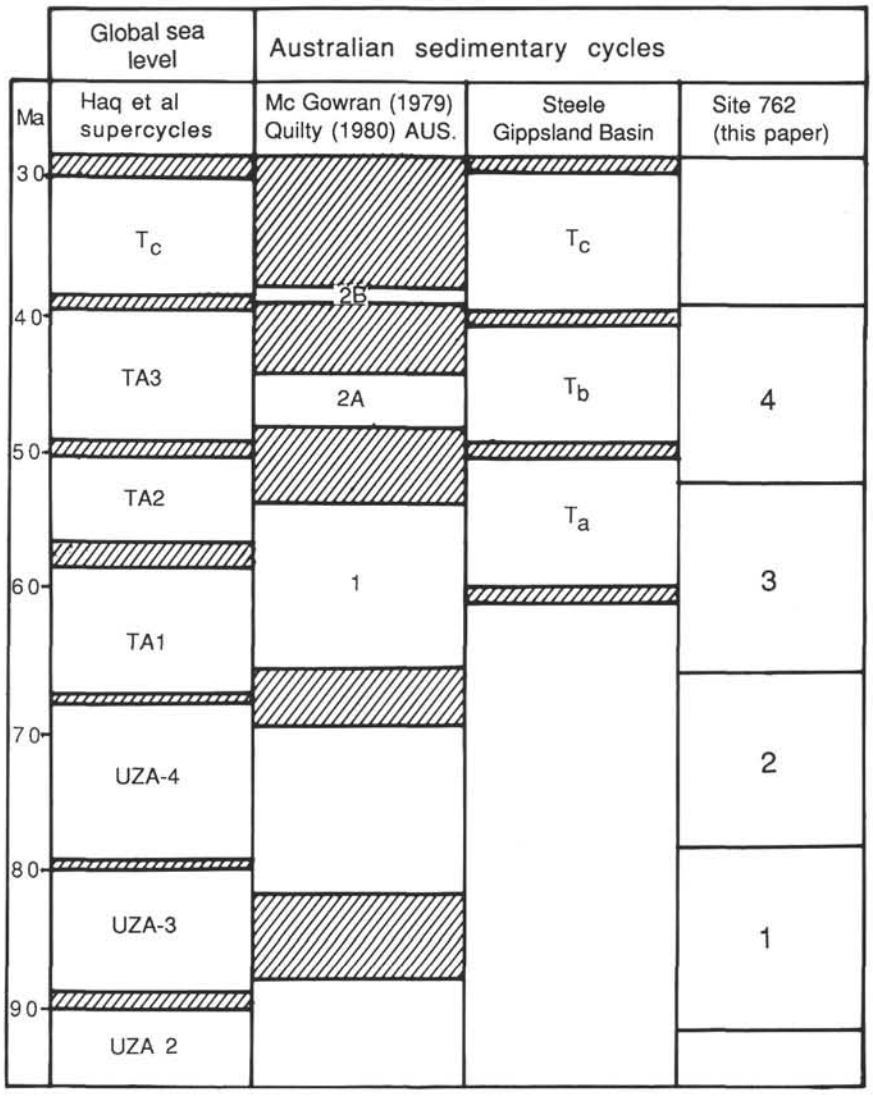

Figure 9. Comparison of duration of hiatuses (diagonal lines) in Australian continental margin sedimentary sequences (McGowran, 1979; Quilty, 1980; Steele, 1976; Golovchenko et al., this chapter) with ages of unconformities separating eustatic sea-level supercycles (Haq et al, 1987). After Loutit and Kennett, 1981.

interesting to note that these large-scale cycles have boundaries that coincide with the Cenomanian/Turonian and Cretaceous/Tertiary boundaries. In addition, the cycle at 51 Ma coincides with the opening of the Tasman Sea and the beginning of seafloor spreading between Australia and Antarctica (Cande and Mutter, 1982; Watts, 1982). A condensed sequence, a major unconformable surface where high volcanic activity hence fast spreading occurred, and a boundary associated with the opening of an ocean gateway all point to tectonism as the primary cause of sea-level change associated with these events.

Ocean gateways and changes in bottom currents that influence dissolution, oxygen content, and preservation of microfossils, along with changes in provenance of sediments, would help explain the changes and alternation of sediments observed.

CONCLUSIONS

1. Core data document the cyclicity of nannofossil and clay abundances, but with uncertain sedimentation rates, it is difficult to identify with any precision any but the 20-k.y. precession and 42-k.y. obliquity cycles.

2. Downhole logs, on the other hand, are able to characterize the nature of the cyclicity in the Eocene through a multitaper spectral analysis technique. The vertical resolution of the log and low sedimentation rates precludes identification of obliquity and precession cycles using this analysis. However, eccentricity cycles of 413-123-95 k.y. are identified from 250 to 365 mbsf. The consistency of the ratios and agreement with predicted ratios supports the identification of the amplitude peaks as eccentricity cycles.

3. The power spectra of the log data from the Mesozoic section have peaks that cannot be correlated with any Milankovitch periods. Core data clearly indicate color cycles with time durations of approximately 20 k.y. and 42 k.y. (precession and obliquity, respectively), but none that can be correlated with eccentricity periods. This indicates that eccentricity may not have played a major role in controlling sedimentation in the Mesozoic.

4. Four low-frequency events are identified at Site 762 from both the log and core data. Nearly continuous pelagic carbonate sedimentation at this site presents a complete picture of minor lithostratigraphic and biostratigraphic changes with time that can be easily recognized. The duration of these cycles averages about 13 m.y. and represents approximately 110–150 m of sediment. The event boundaries, which are not unconformities, correlate well with observed hiatuses in other wells in western Australia and appear to correspond to the timing of supercycle hiatuses postulated by the Vail eustatic curve. However, the event boundaries also correspond in time to regional tectonic events and associated ocean circulation changes, which would indicate that not global but regional events controlled the continental margin sedimentation off western Australia during the Late Cretaceous to Eocene.

ACKNOWLEDGMENTS

We thank the Shipboard Scientific Party of ODP Leg 122 for the cooperative scientific effort that made this project possible. This manuscript benefited from the reviews of R. Anderson, M. Lovell, and anonymous reviewers. Software for some of the log analysis was generously provided by Terrisciences, Inc. Financial support was provided by US-SAC.

REFERENCES

Borella, P. E., 1984. Sedimentary petrology and cyclic sedimentation patterns, Walvis Ridge Transect, Leg 74, Deep Sea Drilling Project. *In* Moore, T. C., Jr., Rabinowitz, P. D., et al., *Init. Repts. DSDP,* 74: Washington (U.S. Govt. Printing Office), 645–662.

Cande, S. C., and Mutter, J. C., 1982. A revised identification of the oldest sea-floor spreading anomalies between Australia and Antarctica. *Earth Planet. Sci. Lett.,* 58:151–160.

Dean, W. E., Gardner, J. V., Jansa, L. F., Copek, P. I., Siebold, E., 1978. Cyclic sedimentation along the continental margin of North Africa. *In* Lancelot, Y., Siebold, E., et al., *Init. Repts. DSDP,* 41: Washington (U.S. Govt. Printing Office), 965–990.

Haq, B. U., Hardenbol, J., and Vail, P. R., 1987. Chronology of fluctuating sea levels since the Triassic. *Science,* 235:1156–1167.

Imbrie, J., and Imbrie, K. P., 1979. *Ice Ages: Solving the Mystery:* New York (Macmillan) and Short Hills, N.J. (Enslow Publications).

Loutit, T. S., and Kennett, J. P., 1981. New Zealand and Australian Cenozoic sedimentary cycles and global sea-level changes. *AAPG Bull.,* 65:1586–1601.

Martini, E., 1971. Standard Tertiary and Quaternary calcareous nannoplankton zonation. *In* Farinacci, A. (Ed.), *Proc. 2nd Planktonic Conf. Roma:* Rome (Ed. Technosci.), 2:739–785.

McGowran, B., 1979. The Tertiary of Australia: foraminiferal overview. *Mar. Micropaleontol.,* 4:235–264.

Milankovitch, M., 1938. Astronomische Mittelzur Erforschung der erdgeschichtlichen Klimate. *Handb. Geophys.,* 9:593–698.

Quilty, P. G., 1977. Cenozoic sedimentation cycles in Western Australia. *Geology,* 5:336–340.

_____, 1980. Sedimentation cycles in the Cretaceous and Cenozoic of Western Australia. *Tectonophysics,* 63:349–366.

Rider, M. H., 1986. *The Geological Interpretation of Well Logs:* New York (Halsted Press).

Roth, P. H., 1978. Cretaceous nannoplankton biostratigraphy and oceanography of the Northwestern Atlantic Ocean. *In* Benson, W. E., Sheridan, R. E., et al., *Init. Repts. DSDP,* 44: Washington (U.S. Govt. Printing Office), 731–759.

Shipboard Scientific Party, 1990. Site 762. *In* Haq, B. U., von Rad, U., et al., *Proc. ODP, Init. Repts.,* 122: College Station, TX (Ocean Drilling Program), 213–288.

Sissingh, W., 1977. Biostratigraphy of Cretaceous calcareous nannoplankton. *Geol. Mijnbouw,* 56:37–65.

Steele, R. J., 1976. Some concepts of seismic stratigraphy with application to the Gippsland Basin. *APEA J.,* 16:67–71.

Thompson, D. J., 1977. Spectrum estimation techniques for characterization and development of WT4 wave grids. *Bell Sept. Tech. J.,* No. 56.

Veevers, J. J., 1988. Morphotectonics of Australia's north-western margin: a review. *In* Purcell, P. G., and Purcell, R. R. (Eds.), *The North West Shelf, Australia:* Proc. Pet. Expl. Soc. Aust. Symp., 19–27.

von Rad, U., Thurow, J., Haq, B. U., Gradstein, F., Ludden, J., and ODP Leg 122/123 Shipboard Scientific Parties, 1989. Triassic to Cenozoic evolution of the NW Australian continental margin and the birth of the Indian Ocean (preliminary results of ODP Legs 122 and 123). *Geol. Rundsch.,* 78:1189–1210.

Watts, A. B., 1982. Tectonic subsidence, flexure and global changes of sea level. *Nature,* 297:469–474.

Date of initial receipt: 4 June 1990
Date of acceptance: 26 March 1991
Ms 122B-141